MATERIALS AND METHODS

Standard Protocol Approvals, Registrations, and Patient Consents

Informed consent was obtained from MS patients and controls in accordance with institutional guidelines and experiments were approved by the ethical board of the Centre Hospitalier de l'Université de Montréal (CHUM research ethic committee approval number BH07.001, 20.332).

Data Availability

The data is freely shared via two interactive R shiny applications available at https://pratlab.shinyapps.io/EAEbrain_10X (total cells)
and https://pratlab.shinyapps.io/EAEbrain_CD31 (CD31-selected cells). ScRNA-seq raw data (FASTQ files) are available to investigators via the GEO accession number GSE199460.

EAE induction and scoring

All animal procedures were approved by the Centre de Recherche du Centre Hospitalier de l'Université de Montreal (CRCHUM) Animal Care committee and followed guidelines of the Canadian Council on Animal Care.

MOG35-55 EAE was induced as previously described (7, 8). Female C57BL/6J mice (the Jackson Laboratory) aged 6 to 10 weeks old were immunized subcutaneously in the regions above the flanks with 200 µg of MOG35-55 (MEVGWYRSPFSRVVHLYRNGK; Alpha Diagnostic) in a 100 µl emulsion of incomplete Freund's adjuvant supplemented with 4 mg/ml Mycobacterium tuberculosis (Fisher Scientific). Pertussis toxin (400 ng, Cedarlane List Biological labs) was injected intraperitoneally 48 hours after EAE induction.

Clinical score: Mice were examined daily for clinical signs of EAE and were scored as followed: 0, unaffected; 1, limp tail; 2, slow righting-reflex; 3, partial hindlimb paralysis; 4, complete hindlimb paralysis; and 5, moribund/death. Animals were sacrificed 14 days after induction; one mouse at a clinical score of 3 and two mice at a clinical score of 4.

Deeply anesthetized mice were transcardially perfused with cold PBS and their brains were recovered and processed for cell isolation.

Tissue dissociation for single-cell RNA-seq

Brain tissue from mice were dissociated into single-cell suspensions by using the Adult Brain Dissociation Kit (Miltenyi Biotec). First, brains were washed in cold PBS and cut in small pieces. The tissues were dissociated into single-cell suspensions by combining 30 minutes of mechanical dissociation at 37°C (using the gentleMACS™ Octo Dissociators) with enzymatic degradation. After the dissociation, the Debris Removal Solution was used to remove the debris. The red blood cell removal step was not performed because the mice were perfused prior to brain removal. Cells were then counted and processed using the Chromium Next GEM Single Cell 5' Library & Gel Bead Kit v1.1 (10X Genomics).

Endothelial cell enrichment

Brain endothelial cells were isolated using the CD31 MicroBead Kit and MACS isolation columns (positive selection) according to the manufacturer's protocol (Miltenyi Biotec). Endothelial cells were counted and similarly processed using the Chromium Next GEM single cell 5' library and gel bead kit v1.1 (10X Genomics).

scRNA-seq amplification, library preparation and sequencing

Single cell libraries were generated using the Chromium Next GEM single cell 5' library and gel bead kit v1.1 according to the manufacturer's protocol (10X genomics). Briefly, the samples containing 10.000 cells were partitioned into nanoliter-scale Gel Beads-in-emulsion (GEMs) using the Chromium Controller. Then, single cell GEMs underwent reverse transcription. Each GEM contains a unique barcode meaning that after the RT reaction, all the cDNA from each individual cells share a common barcode. Barcoded cDNA was amplified via PCR with primers against common 5' and 3' ends added during

the RT. Libraries were sequenced and the barcodes were used to separately index each cell's transcriptome.

Data analysis

Preprocessing

Single-cell fastqs files were processed with cellranger and filtered matrices were imported in R with the *Seurat*[33] package. All statistical and further analysis were conducted in R. scRNA-seq data was normalized with the SCTransform method (*Seurat*) and clustered with the Louvain algorithm. 15 principal components were used for the UMAP reduction. Batch-correction was needed since samples were sequenced in two distinct batches on the flowcells. Therefore, samples from the same flowcell were concatenated using the merge function in *Seurat*. The two batches were then integrated using *Seurat*'s SCT anchoring workflow.

Marker Identification and cell-type proportions

Molecular markers were identified with the *MAST* method, and clusters were merged into a cell-type when deemed biologically relevant. For cell-types found in both EAE and CTL mice, the *FindConservedMarkers* function (*Seurat*[33]) was used. This allowed to compare fold-changes and p-values across both conditions. For the immune cells (which were predominantly found in EAE animals), the standard FindAllMarkers function (Seurat) was applied. Only positive fold-changes with adjusted p-value<0.01 were identified as cell markers. In all cases, the sequencing batch was added as a latent variable to alleviate any batch effect in the identification of markers. The extensive lists of cell-type markers can be explored on the shiny apps and are provided as supplementary tables. The relative ratios for each cell-type were calculated by first finding the proportion of each population for every sample. Secondly, the sample ratios for a given cell-type are normalized by the sum, to compare the relative importance of the population between samples.

Differential Expression Analysis

Since immune subsets were mostly absent from the control samples, differential expression analysis was only conducted within the CNS-resident clusters (ie; microglia, ECs, MOLs, astrocytes, ependymal cells, choroid plexus cells, pericytes, fibroblast, neuroblast, and neurons). Using the batch as a latent variable, the DESeq2 method [34] was used to generate average fold-changes and adjusted p-values. Genes were considered differentially expressed (DEGs) when log2(FC)>.5 and FDR<0.05. The extensive lists of differentially expressed genes by across cell-types can be explored on the shiny apps and are provided as supplementary tables. Gene set enrichments were conducted using *enrichR* available databases and a fisher test approach using detected genes as background. Since Gene Ontology and KEGG are amongst the most used, we focused on these for the main results. *ClueGO*[35], a *Cytoscape* plugin, was used to present a network view of the enriched ontologies.

Pseudotime

To identify the continuous arteriovenous architecture in the CD31 selected single-cell data, we used the integration workflow at the sample level. This allowed to use *slingshot*[36], a R package that provide means to perform pseudotime analysis. Using arterial ECs as a root, this produced 2 continuous trajectories (1) going from arterial ECs to venous ECs going through the capillaries and (2) from arterial ECs to venous ECs going through interferon ECs. We then used a random forest algorithm on the top 300 highly variable genes (implemented in the *tidyverse*[37] R package). This allowed to identify genes associated with the pseudotime trajectory. We reported the top 5% of the tested genes contributing the most to the outcome as supplementary material.

Identifying Potential Interactions

Immune subsets were characterized by identifying common transcriptional signatures, and further characterizing the specific expression profiles of each cell population. To further investigate possible interactions between immune subsets and endothelial cells, we used *CellChat*[32], a tool to infer possible ligand-receptors interactions in single-cell data. This allowed analyses of ubiquitous and cell-type specific potential of infiltration through interaction with the cellular lining of the BBB.

Immunofluorescence staining

Human brain tissue was obtained from patients diagnosed with clinical and neuropathological MS diagnosis according to the revised 2010 McDonald's criteria (CHUM research ethic committee approval number BH07.001, 20.332). Tissue samples were collected from 3 control donors (42- , 67-year-old males; 34-years-old female) and 3 MS patients (33- and 44-years old females with relapsing-remitting MS; 61-years old male with secondary progressive MS) with full ethical approval and informed consent as approved by the local ethics committee. Frozen brain tissues were sectioned into slices (7 µm) and lesion identification was performed using Luxol Fast Blue/Haematoxylin & Eosin staining and Oil Red O staining as previously published [38–40].

Slides were fixed in acetone for 10 min, transferred to ethanol for 5 min, hydrated in PBS, and blocked with 10% species-specific serum of the secondary antibody hosts. Sections were incubated for 1h at room temperature with primary antibodies diluted in 3% species-specific serum. Primary antibodies were revealed by using secondary antibodies linked to AF488 or Cy3 (Jackson ImmunoResearch, dilution 1/600, incubated 40 min at room temperature). Sections were then mounted using Mowiol reagent containing TO-PRO®3 (Thermo Fisher Scientific, 1:400). The following primary antibodies were used: mouse anti-human DARC (1/30; R&D Systems), goat anti-human lipocalin-2 (1/20, R&D Systems), rabbit anti-human caveolin-1 (1/250; abcam).

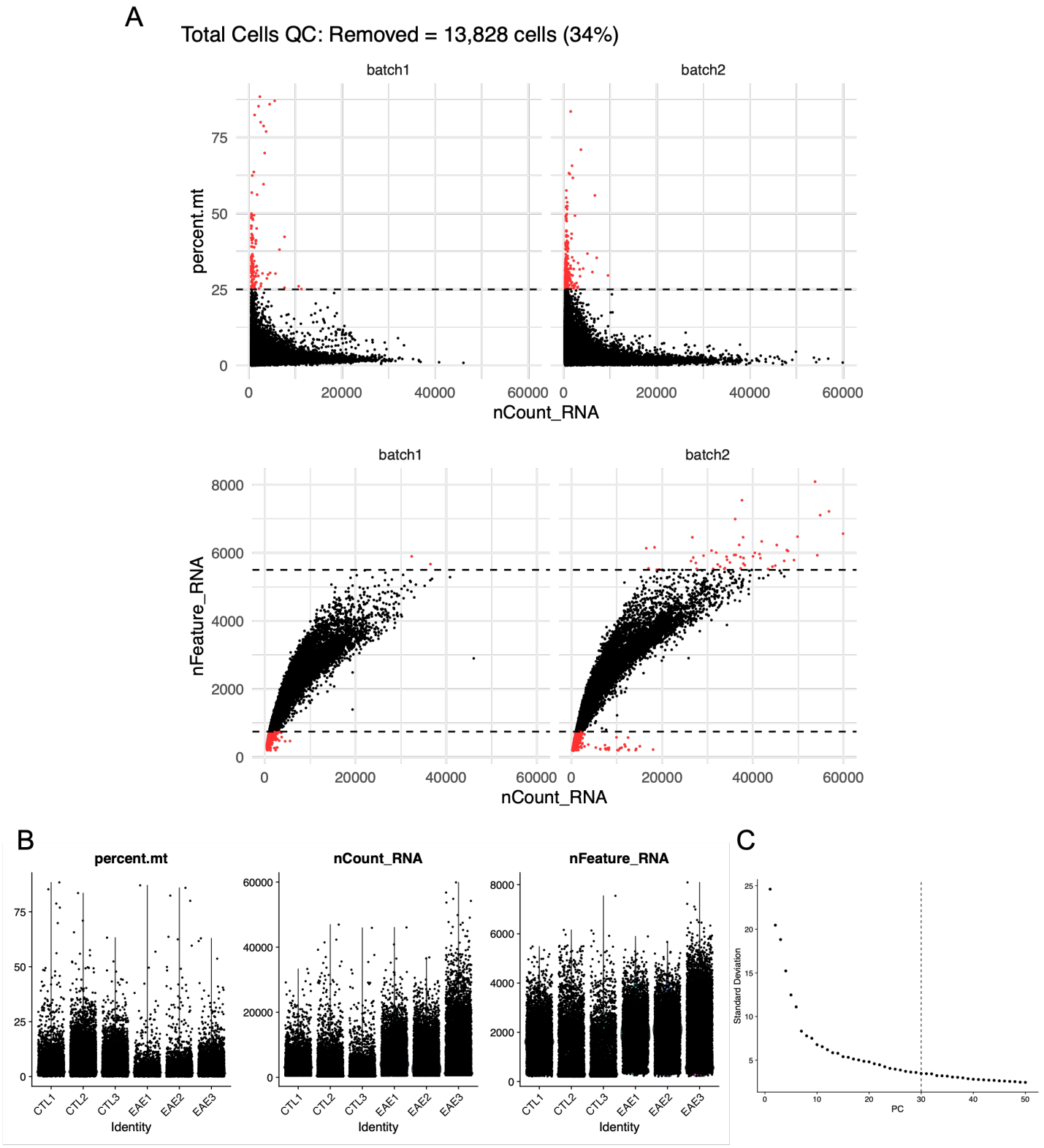
A
Total Cells QC: Removed = 13,828 cells (34%)
batch1
batch2
percent.mt
nCount_RNA
nFeature_RNA
B
percent.mt
nCount_RNA
nFeature_RNA
CTL1
CTL2
CTL3
EAE1
EAE2
EAE3
Identity
C
Standard Deviation
PC

eFigure 1

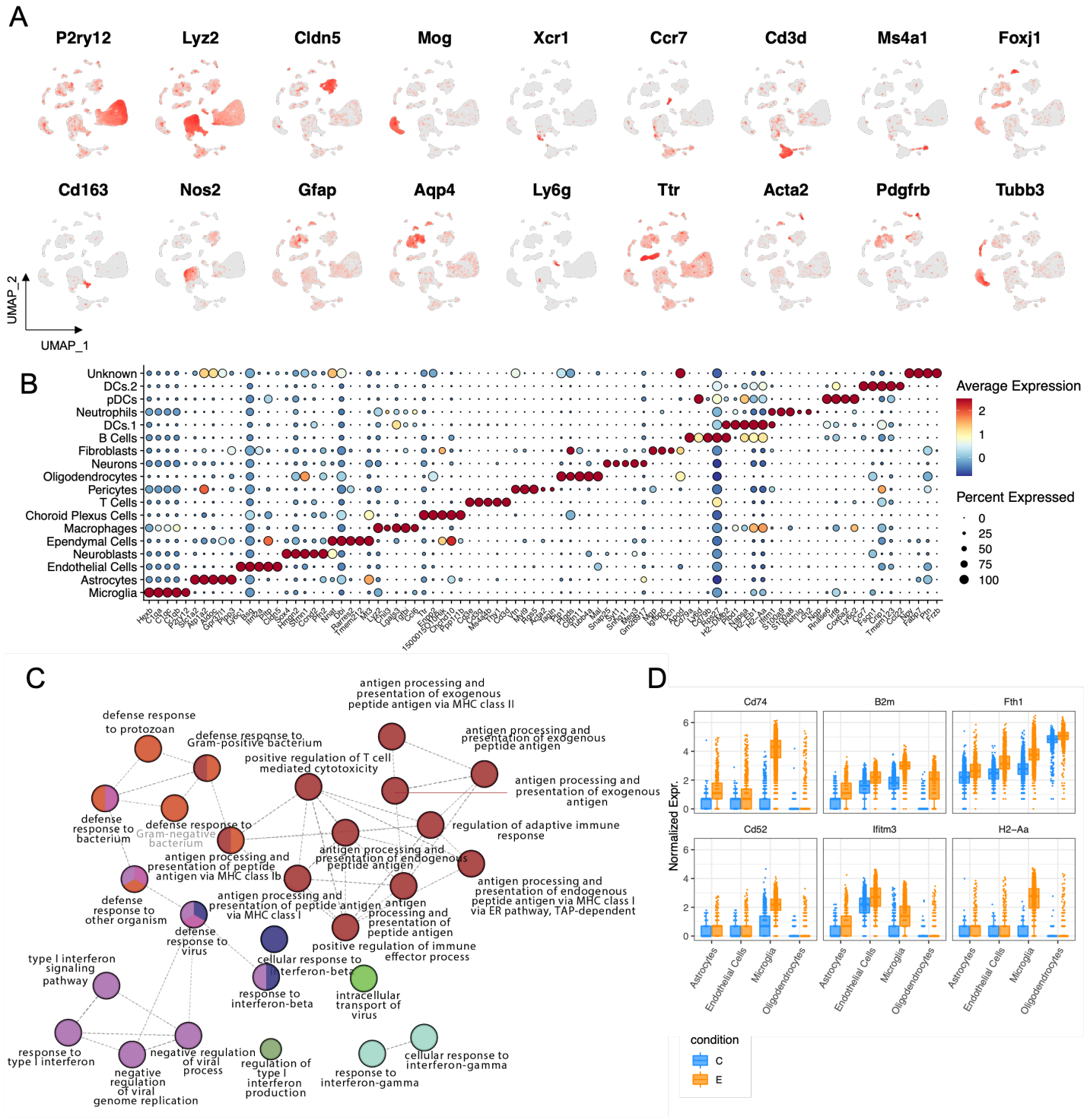
A
P2ry12
Lyz2
Cldn5
Mog
Xcr1
Ccr7
Cd3d
Ms4a1
Foxj1
Cd163
Nos2
Gfap
Aqp4
Ly6g
Ttr
Acta2
Pdgfrb
Tubb3
UMAP_2
UMAP_1
B
Unknown
DCs.2
pDCs
Neutrophils
DCs.1
B Cells
Fibroblasts
Neurons
Oligodendrocytes
Pericytes
T Cells
Choroid Plexus Cells
Macrophages
Ependymal Cells
Neuroblasts
Endothelial Cells
Astrocytes
Microglia
Average Expression
2
1
0
Percent Expressed
0
25
50
75
100
C
antigen processing and presentation of exogenous peptide antigen via MHC class II
defense response to protozoan
defense response to Gram-positive bacterium
positive regulation of T cell mediated cytotoxicity
antigen processing and presentation of exogenous peptide antigen
antigen processing and presentation of exogenous antigen
defense response to bacterium
defense response to Gram-negative bacterium
regulation of adaptive immune response
antigen processing and presentation of peptide antigen via MHC class Ib
antigen processing and presentation of endogenous peptide antigen
antigen processing and presentation of endogenous peptide antigen via MHC class I via ER pathway, TAP-dependent
defense response to other organism
antigen processing and presentation of peptide antigen via MHC class I
defense response to virus
antigen processing and presentation of peptide antigen
positive regulation of immune effector process
cellular response to interferon-beta
type I interferon signaling pathway
response to interferon-beta
intracellular transport of virus
response to type I interferon
negative regulation of viral process
negative regulation of viral genome replication
regulation of type I interferon production
response to interferon-gamma
cellular response to interferon-gamma
D
Cd74
B2m
Fth1
Cd52
Ifitm3
H2−Aa
Normalized Expr.
Astrocytes
Endothelial Cells
Microglia
Oligodendrocytes
condition
C
E

eFigure 2

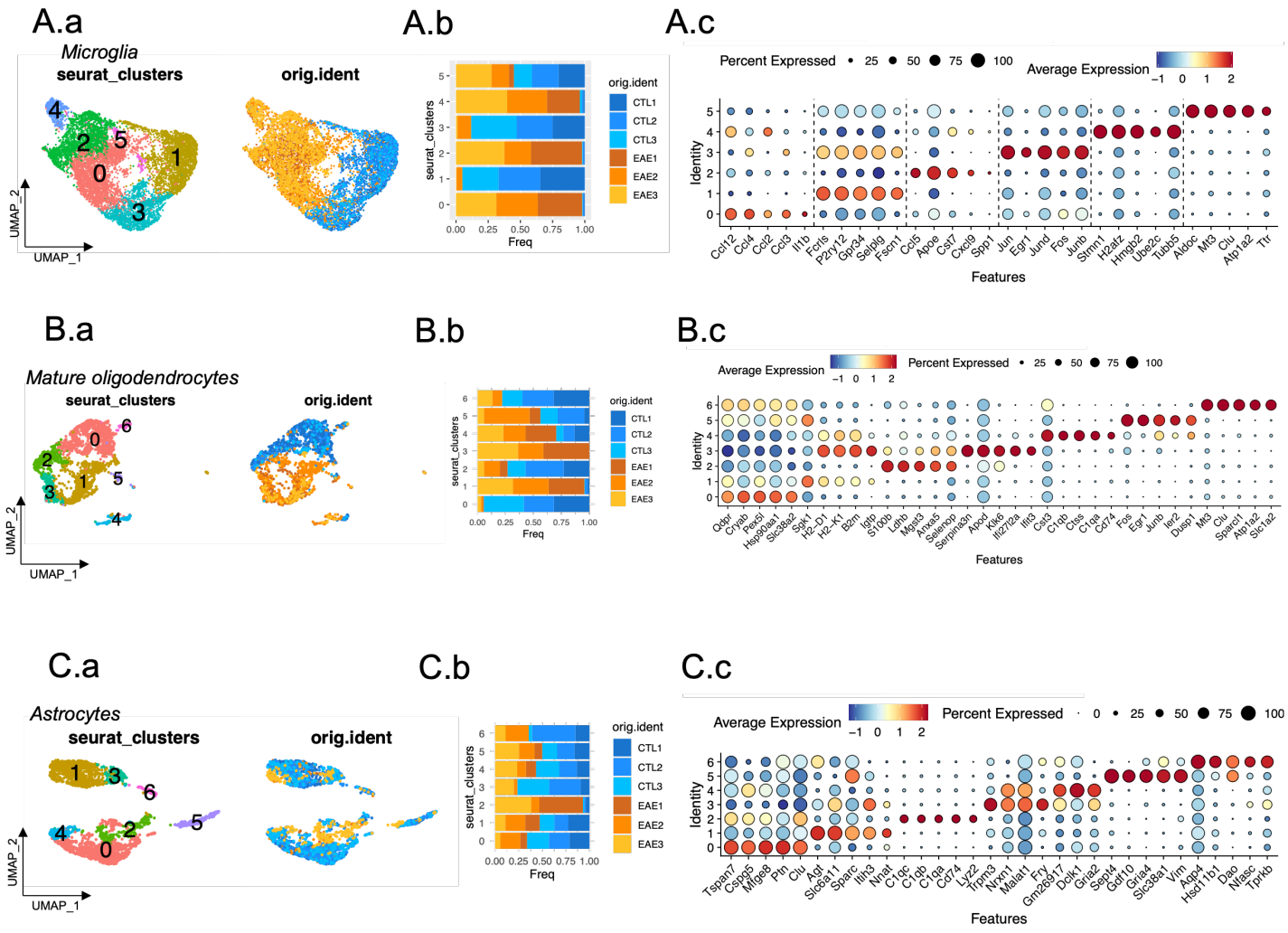
A.a
Microglia
seurat_clusters
orig.ident
UMAP_2
UMAP_1
A.b
seurat_clusters
Freq
orig.ident
CTL1
CTL2
CTL3
EAE1
EAE2
EAE3
A.c
Percent Expressed
Average Expression
Identity
Features
B.a
Mature oligodendrocytes
seurat_clusters
orig.ident
B.b
B.c
C.a
Astrocytes
C.b
C.c

eFigure 3

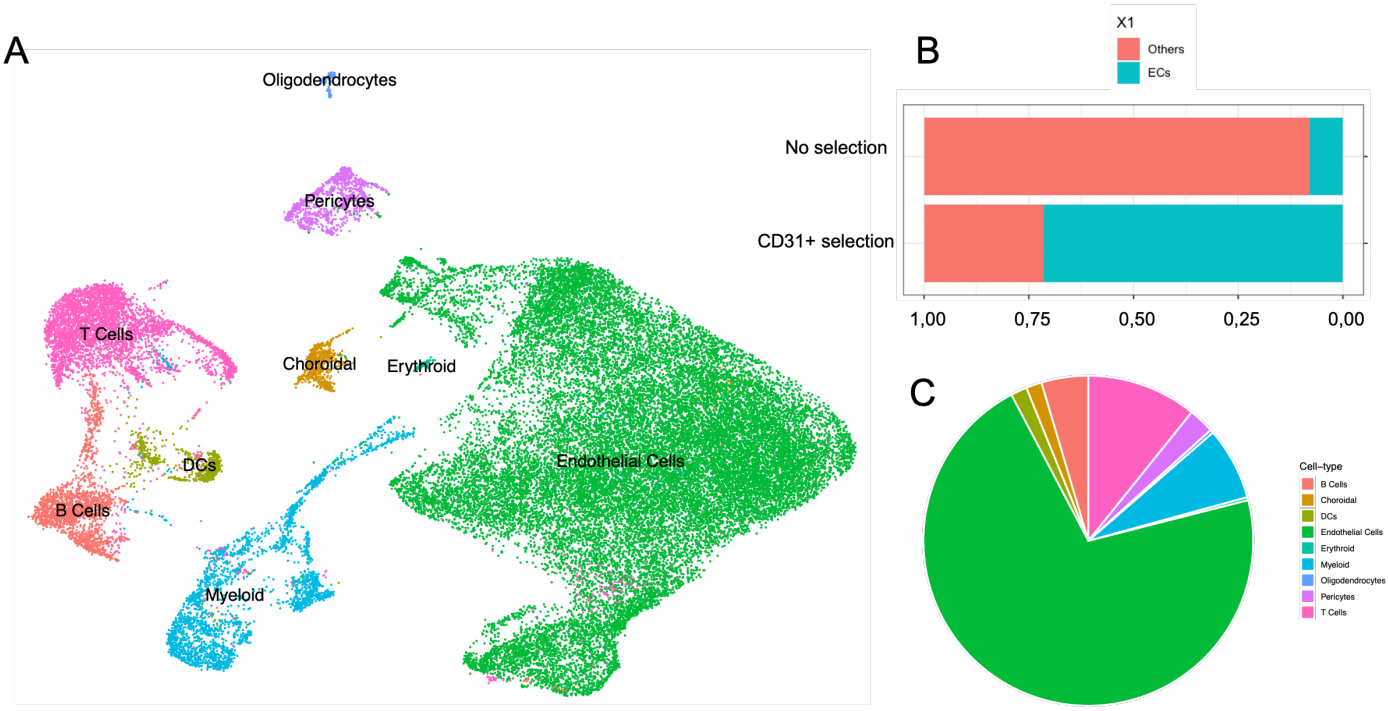
A
Oligodendrocytes
Pericytes
T Cells
Choroidal
Erythroid
DCs
Endothelial Cells
B Cells
Myeloid
B
X1
Others
ECs
No selection
CD31+ selection
1,00
0,75
0,50
0,25
0,00
C
Cell–type
B Cells
Choroidal
DCs
Endothelial Cells
Erythroid
Myeloid
Oligodendrocytes
Pericytes
T Cells

eFigure 4

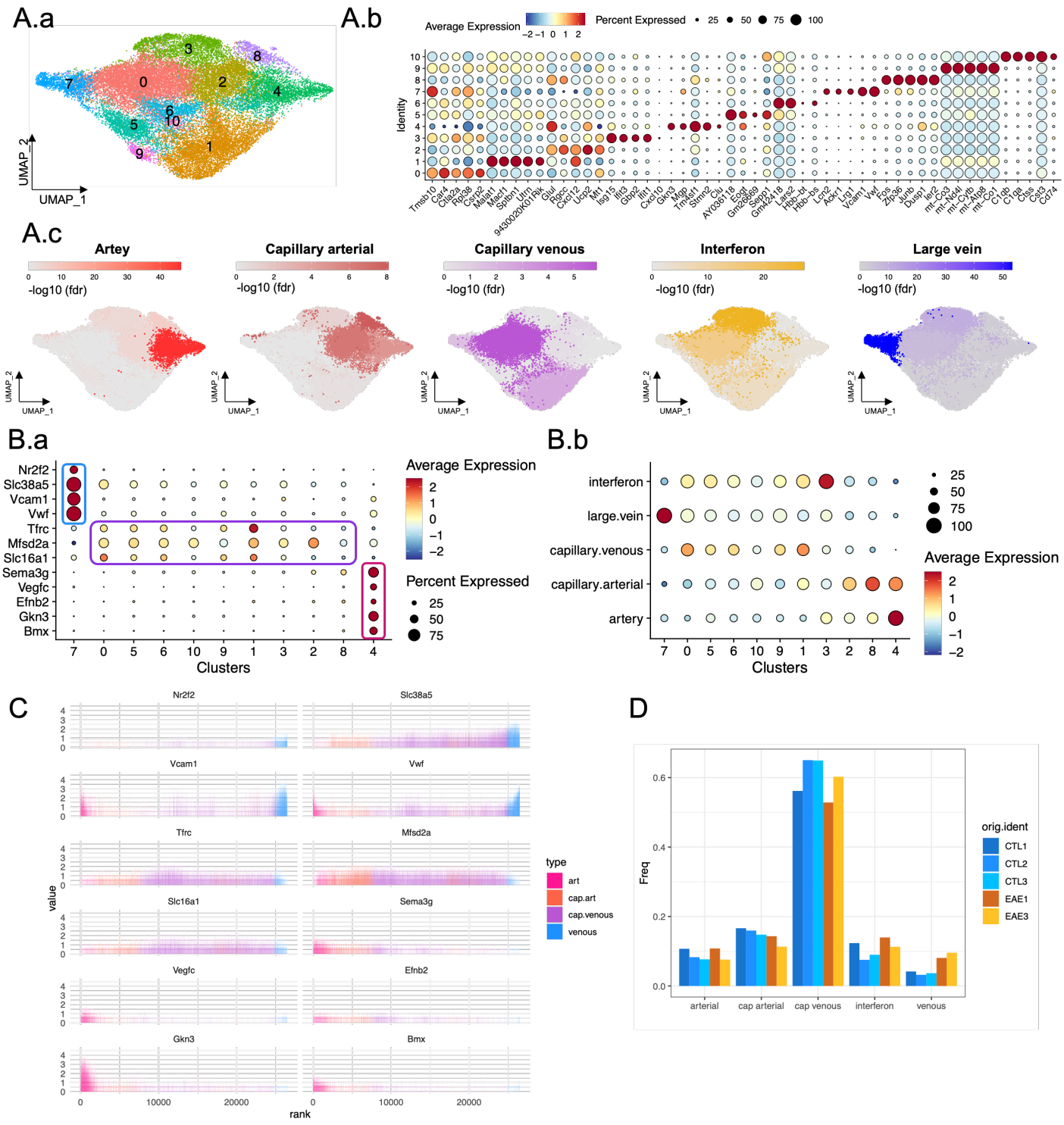
A.a
A.b
A.c
Artey
Capillary arterial
Capillary venous
Interferon
Large vein
-log10 (fdr)
B.a
B.b
Average Expression
Percent Expressed
Clusters
interferon
large.vein
capillary.venous
capillary.arterial
artery
C
D
type
art
cap.art
cap.venous
venous
rank
value
orig.ident
CTL1
CTL2
CTL3
EAE1
EAE3
Freq
arterial
cap arterial
cap venous
interferon
venous

eFigure 5

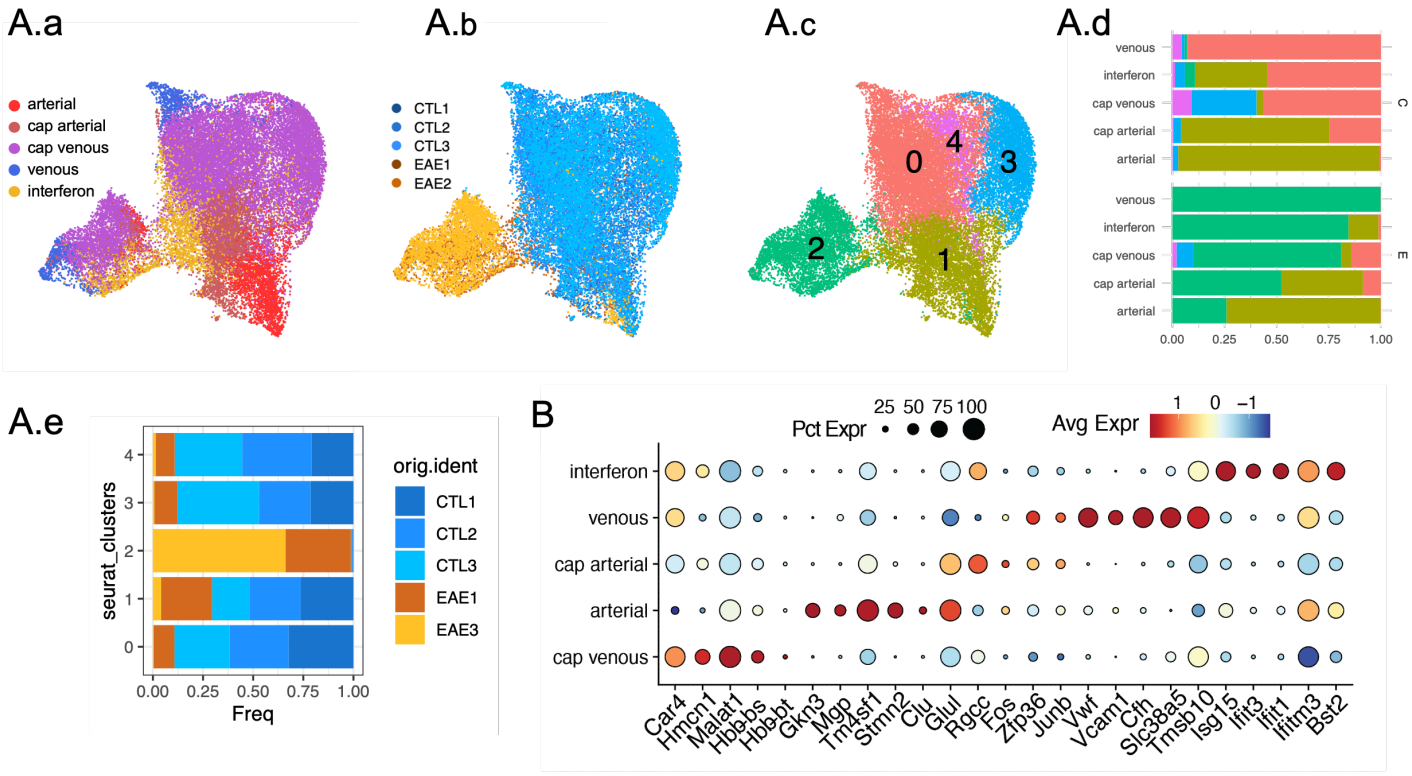
A.a
arterial
cap arterial
cap venous
venous
interferon
A.b
CTL1
CTL2
CTL3
EAE1
EAE2
A.c
0
1
2
3
4
A.d
venous
interferon
cap venous
cap arterial
arterial
0.00
0.25
0.50
0.75
1.00
A.e
seurat_clusters
Freq
orig.ident
CTL1
CTL2
CTL3
EAE1
EAE3
B
Pct Expr
25 50 75 100
Avg Expr
1 0 −1
interferon
venous
cap arterial
arterial
cap venous
Car4
Hmcn1
Malat1
Hba-bs
Hba-bt
Gkn3
Mgp
Tm4sf1
Stmn2
Clu
Glul
Rgcc
Fos
Zfp36
Junb
Vwf
Vcam1
Cfh
Slc38a5
Tmsb10
Isg15
Ifit3
Ifit1
Ifitm3
Bst2
C.a
common
RESPONSE TO TYPE I INTERFERON
INTERFERON GAMMA MEDIATED SIGNALING PATHWAY
RESPONSE TO CYTOKINE
CYTOKINE MEDIATED SIGNALING PATHWAY
RESPONSE TO INTERFERON GAMMA
ANTIGEN PROCESSING AND PRESENTATION OF ENDOGENOUS ANTIGEN
DEFENSE RESPONSE
ANTIGEN PROCESSING AND PRESENTATION OF ENDOGENOUS PEPTIDE ANTIGEN
ANTIGEN PROCESSING AND PRESENTATION OF PEPTIDE ANTIGEN
ANTIGEN PROCESSING AND PRESENTATION OF PEPTIDE ANTIGEN VIA MHC CLASS IB
ANTIGEN PROCESSING AND PRESENTATION OF EXOGENOUS PEPTIDE ANTIGEN VIA MHC CLASS I TAP INDEPENDENT
ANTIGEN PROCESSING AND PRESENTATION
INNATE IMMUNE RESPONSE
ANTIGEN PROCESSING AND PRESENTATION OF EXOGENOUS PEPTIDE ANTIGEN VIA MHC CLASS I
ANTIGEN PROCESSING AND PRESENTATION VIA MHC CLASS IB
0
5
10
15
C.b
veins
REGULATION OF CELLULAR COMPONENT MOVEMENT
RESPONSE TO MOLECULE OF BACTERIAL ORIGIN
RESPONSE TO CYTOKINE1
BIOLOGICAL ADHESION
TISSUE MIGRATION
CELL MOTILITY
AMEBOIDAL TYPE CELL MIGRATION
INFLAMMATORY RESPONSE
RESPONSE TO BIOTIC STIMULUS
EXOCYTOSIS
ENDOTHELIAL CELL MIGRATION
RESPONSE TO BACTERIUM
CELLULAR RESPONSE TO BIOTIC STIMULUS
REGULATION OF EPITHELIAL CELL MIGRATION
OXIDATIVE PHOSPHORYLATION
0
1
2
3
−log10(fdr)

eFigure 6

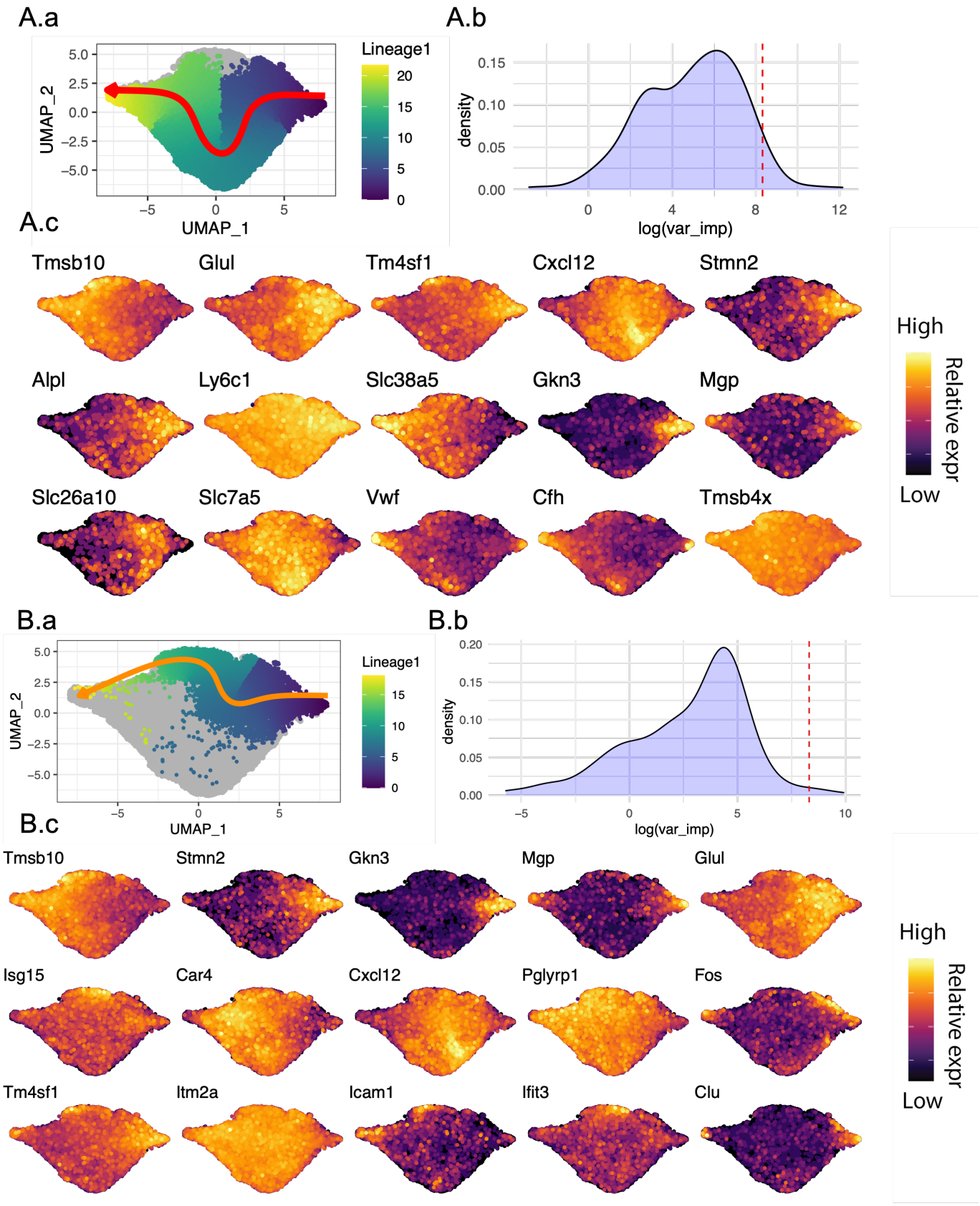
A.a
A.b
A.c
UMAP_2
UMAP_1
Lineage1
density
log(var_imp)
Tmsb10
Glul
Tm4sf1
Cxcl12
Stmn2
Alpl
Ly6c1
Slc38a5
Gkn3
Mgp
Slc26a10
Slc7a5
Vwf
Cfh
Tmsb4x
High
Relative expr
Low
B.a
B.b
B.c
Isg15
Car4
Pglyrp1
Fos
Itm2a
Icam1
Ifit3
Clu

eFigure 7


A
Normalized expression
Vcam1
Icam1
Fn1
Selp
Sele
Cldn5
Ocln
F11r
Tjp1
Cdh5
2.5
0.0
−2.5
−5.0
A
V
EAE
Control
B
CAMs
TJMs
Vcam1
Selp
Sele
Icam1
Fn1
Tjp1
Ocln
F11r
Cldn5
Cdh5
***
**
arterial
cap arterial
cap venous
interferon
venous
value
2
1
0

eFigure 8

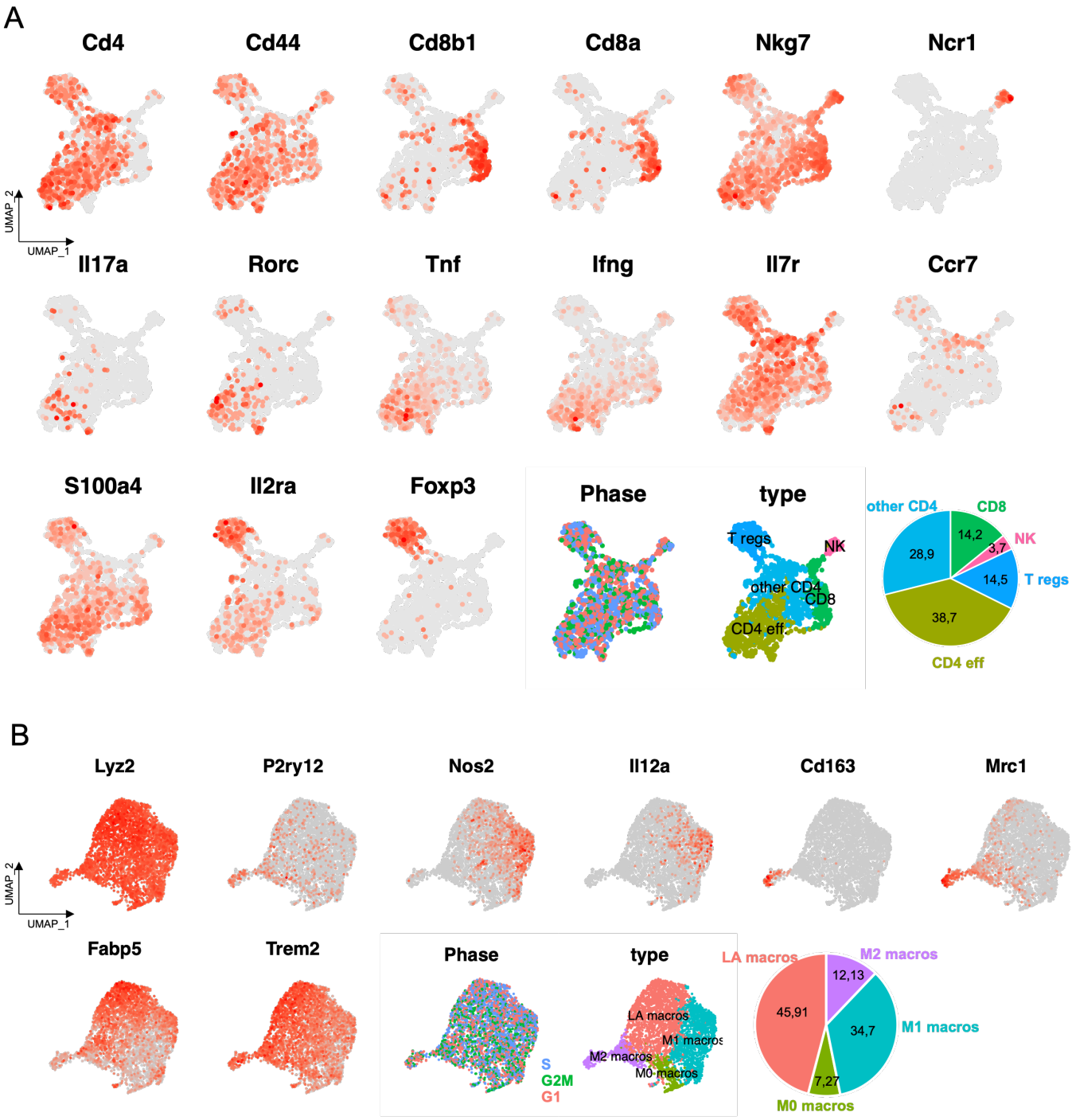
A
Cd4
Cd44
Cd8b1
Cd8a
Nkg7
Ncr1
UMAP_2
UMAP_1
Il17a
Rorc
Tnf
Ifng
Il7r
Ccr7
S100a4
Il2ra
Foxp3
Phase
type
T regs
NK
other CD4
CD8
CD4 eff
other CD4
CD8
NK
T regs
CD4 eff
14,2
3,7
28,9
14,5
38,7
B
Lyz2
P2ry12
Nos2
Il12a
Cd163
Mrc1
Fabp5
Trem2
Phase
type
S
G2M
G1
LA macros
M1 macros
M2 macros
M0 macros
LA macros
M2 macros
M1 macros
M0 macros
12,13
45,91
34,7
7,27

eFigure 9

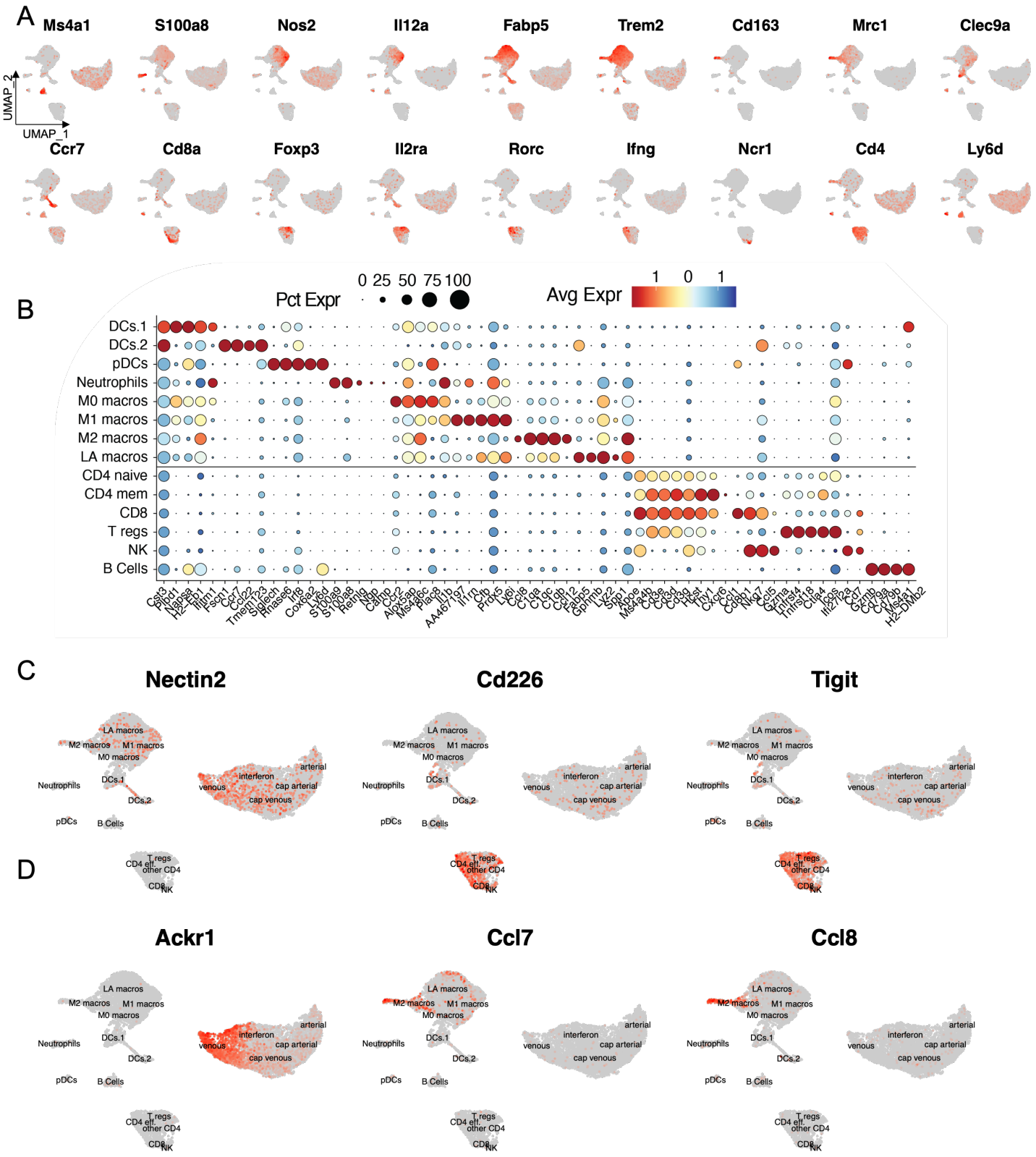
A
Ms4a1
S100a8
Nos2
Il12a
Fabp5
Trem2
Cd163
Mrc1
Clec9a
UMAP_2
UMAP_1
Ccr7
Cd8a
Foxp3
Il2ra
Rorc
Ifng
Ncr1
Cd4
Ly6d
B
Pct Expr
0 25 50 75 100
Avg Expr
1 0 1
DCs.1
DCs.2
pDCs
Neutrophils
M0 macros
M1 macros
M2 macros
LA macros
CD4 naive
CD4 mem
CD8
T regs
NK
B Cells
C
Nectin2
Cd226
Tigit
LA macros
M2 macros
M1 macros
M0 macros
Neutrophils
DCs.1
DCs.2
pDCs
B Cells
arterial
interferon
venous
cap arterial
cap venous
D
T regs
CD4 eff.
other CD4
CD8
NK
Ackr1
Ccl7
Ccl8

eFigure 10

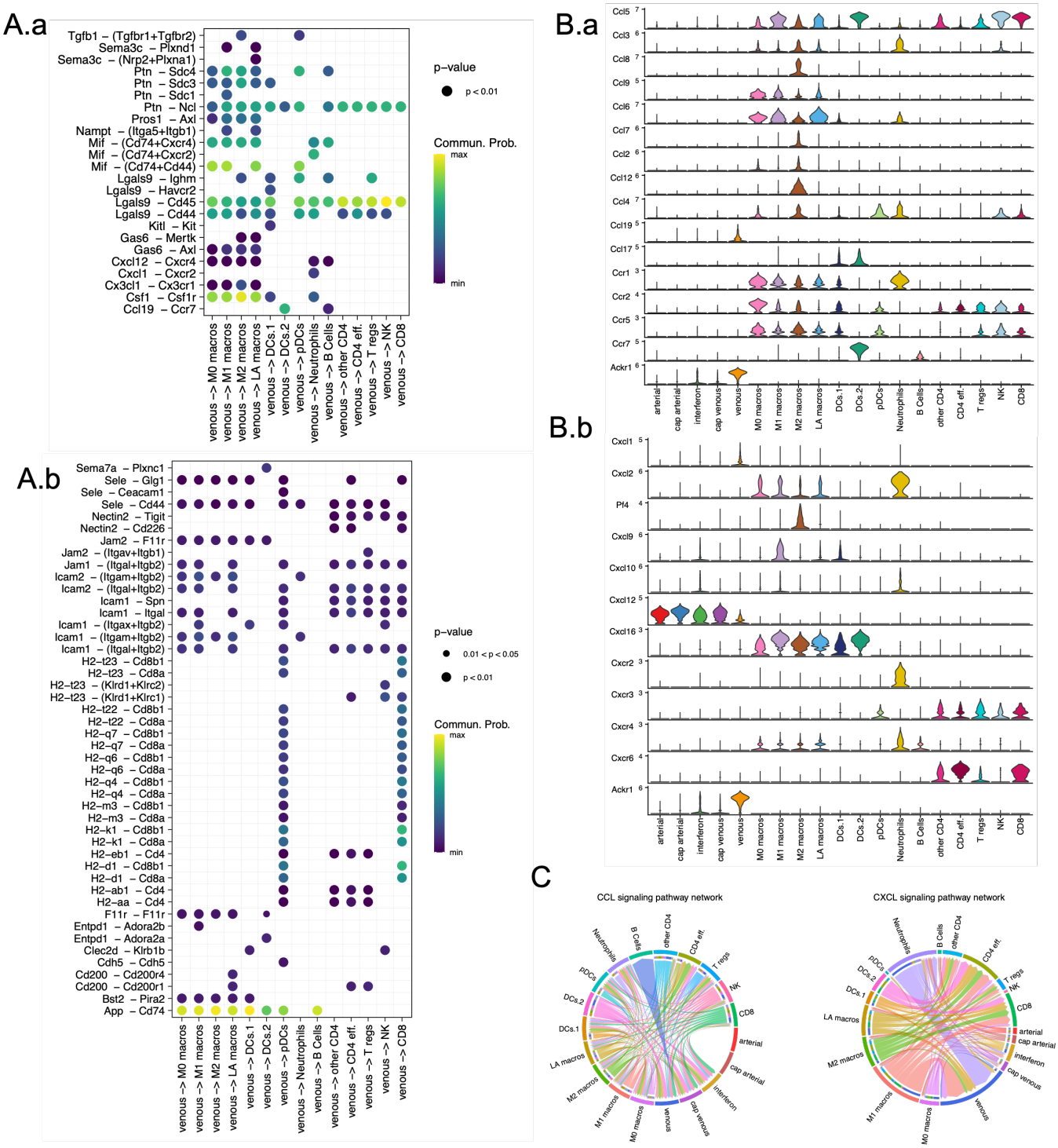
A.a
Tgfb1 – (Tgfbr1+Tgfbr2)
Sema3c – Plxnd1
Sema3c – (Nrp2+Plxna1)
Ptn – Sdc4
Ptn – Sdc3
Ptn – Sdc1
Ptn – Ncl
Pros1 – Axl
Nampt – (Itga5+Itgb1)
Mif – (Cd74+Cxcr4)
Mif – (Cd74+Cxcr2)
Mif – (Cd74+Cd44)
Lgals9 – Ighm
Lgals9 – Havcr2
Lgals9 – Cd45
Lgals9 – Cd44
Kitl – Kit
Gas6 – Mertk
Gas6 – Axl
Cxcl12 – Cxcr4
Cxcl1 – Cxcr2
Cx3cl1 – Cx3cr1
Csf1 – Csf1r
Ccl19 – Ccr7
venous -> M0 macros
venous -> M1 macros
venous -> M2 macros
venous -> LA macros
venous -> DCs.1
venous -> DCs.2
venous -> pDCs
venous -> Neutrophils
venous -> B Cells
venous -> other CD4
venous -> CD4 eff.
venous -> T regs
venous -> NK
venous -> CD8
p–value
p < 0.01
Commun. Prob.
max
min
A.b
Sema7a – Plxnc1
Sele – Glg1
Sele – Ceacam1
Sele – Cd44
Nectin2 – Tigit
Nectin2 – Cd226
Jam2 – F11r
Jam2 – (Itgav+Itgb1)
Jam1 – (Itgal+Itgb2)
Icam2 – (Itgam+Itgb2)
Icam2 – (Itgal+Itgb2)
Icam1 – Spn
Icam1 – Itgal
Icam1 – (Itgax+Itgb2)
Icam1 – (Itgam+Itgb2)
Icam1 – (Itgal+Itgb2)
H2–t23 – Cd8b1
H2–t23 – Cd8a
H2–t23 – (Klrd1+Klrc2)
H2–t23 – (Klrd1+Klrc1)
H2–t22 – Cd8b1
H2–t22 – Cd8a
H2–q7 – Cd8b1
H2–q7 – Cd8a
H2–q6 – Cd8b1
H2–q6 – Cd8a
H2–q4 – Cd8b1
H2–q4 – Cd8a
H2–m3 – Cd8b1
H2–m3 – Cd8a
H2–k1 – Cd8b1
H2–k1 – Cd8a
H2–eb1 – Cd4
H2–d1 – Cd8b1
H2–d1 – Cd8a
H2–ab1 – Cd4
H2–aa – Cd4
F11r – F11r
Entpd1 – Adora2b
Entpd1 – Adora2a
Clec2d – Klrb1b
Cdh5 – Cdh5
Cd200 – Cd200r4
Cd200 – Cd200r1
Bst2 – Pira2
App – Cd74
venous -> M0 macros
venous -> M1 macros
venous -> M2 macros
venous -> LA macros
venous -> DCs.1
venous -> DCs.2
venous -> pDCs
venous -> Neutrophils
venous -> B Cells
venous -> other CD4
venous -> CD4 eff.
venous -> T regs
venous -> NK
venous -> CD8
p–value
0.01 < p < 0.05
p < 0.01
Commun. Prob.
max
min
B.a
Ccl5
Ccl3
Ccl8
Ccl9
Ccl6
Ccl7
Ccl2
Ccl12
Ccl4
Ccl19
Ccl17
Ccr1
Ccr2
Ccr5
Ccr7
Ackr1
arterial
cap arterial
interferon
cap venous
venous
M0 macros
M1 macros
M2 macros
LA macros
DCs.1
DCs.2
pDCs
Neutrophils
B Cells
other CD4
CD4 eff.
T regs
NK
CD8
B.b
Cxcl1
Cxcl2
Pf4
Cxcl9
Cxcl10
Cxcl12
Cxcl16
Cxcr2
Cxcr3
Cxcr4
Cxcr6
Ackr1
arterial
cap arterial
interferon
cap venous
venous
M0 macros
M1 macros
M2 macros
LA macros
DCs.1
DCs.2
pDCs
Neutrophils
B Cells
other CD4
CD4 eff.
T regs
NK
CD8
C
CCL signaling pathway network
CXCL signaling pathway network
Neutrophils
B Cells
other CD4
CD4 eff.
T regs
NK
CD8
arterial
cap arterial
interferon
cap venous
venous
M0 macros
M1 macros
M2 macros
LA macros
DCs.1
DCs.2
pDCs

eFigure 11

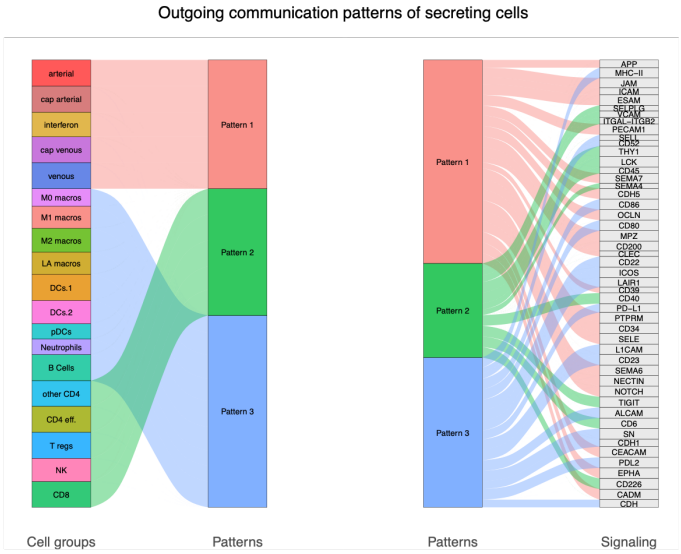
Outgoing communication patterns of secreting cells
arterial
cap arterial
interferon
cap venous
venous
M0 macros
M1 macros
M2 macros
LA macros
DCs.1
DCs.2
pDCs
Neutrophils
B Cells
other CD4
CD4 eff.
T regs
NK
CD8
Pattern 1
Pattern 2
Pattern 3
APP
MHC−II
JAM
ICAM
ESAM
SELPLG
VCAM
ITGAL−ITGB2
PECAM1
SELL
CD52
THY1
LCK
CD45
SEMA7
SEMA4
CDH5
CD86
OCLN
CD80
MPZ
CD200
CLEC
CD22
ICOS
LAIR1
CD39
CD40
PD−L1
PTPRM
CD34
SELE
L1CAM
CD23
SEMA6
NECTIN
NOTCH
TIGIT
ALCAM
CD6
SN
CDH1
CEACAM
PDL2
EPHA
CD226
CADM
CDH
Cell groups
Patterns
Patterns
Signaling

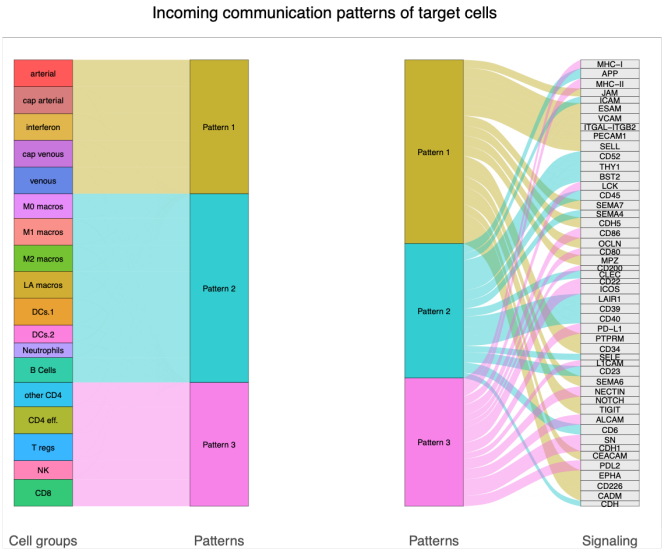
Incoming communication patterns of target cells
arterial
cap arterial
interferon
cap venous
venous
M0 macros
M1 macros
M2 macros
LA macros
DCs.1
DCs.2
Neutrophils
B Cells
other CD4
CD4 eff.
T regs
NK
CD8
Pattern 1
Pattern 2
Pattern 3
MHC−I
APP
MHC−II
JAM
ICAM
ESAM
VCAM
ITGAL−ITGB2
PECAM1
SELL
CD52
THY1
BST2
LCK
CD45
SEMA7
SEMA4
CDH5
CD86
OCLN
CD80
MPZ
CD200
CLEC
CD22
ICOS
LAIR1
CD39
CD40
PD−L1
PTPRM
CD34
SELE
L1CAM
CD23
SEMA6
NECTIN
NOTCH
TIGIT
ALCAM
CD6
SN
CDH1
CEACAM
PDL2
EPHA
CD226
CADM
CDH
Cell groups
Patterns
Patterns
Signaling

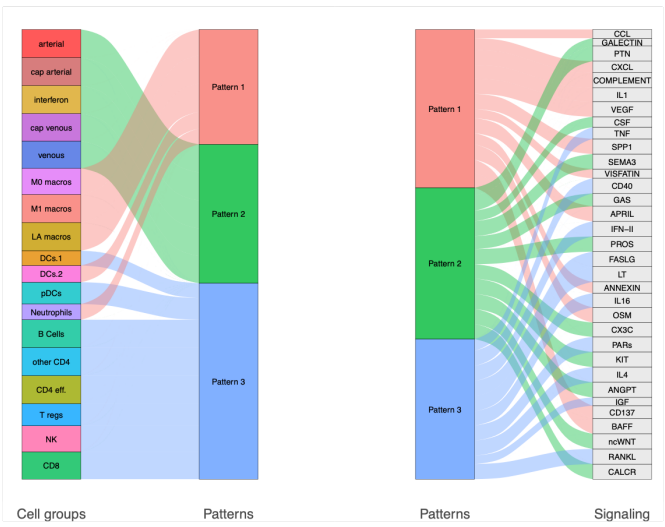
Outgoing communication patterns of secreting cells
arterial
cap arterial
interferon
cap venous
venous
M0 macros
M1 macros
LA macros
DCs.1
DCs.2
pDCs
Neutrophils
B Cells
other CD4
CD4 eff.
T regs
NK
CD8
Pattern 1
Pattern 2
Pattern 3
CCL
GALECTIN
PTN
CXCL
COMPLEMENT
IL1
VEGF
CSF
TNF
SPP1
SEMA3
VISFATIN
CD40
GAS
APRIL
IFN−II
PROS
FASLG
LT
ANNEXIN
IL16
OSM
CX3C
PARs
KIT
IL4
ANGPT
IGF
CD137
BAFF
ncWNT
RANKL
CALCR
Cell groups
Patterns
Patterns
Signaling

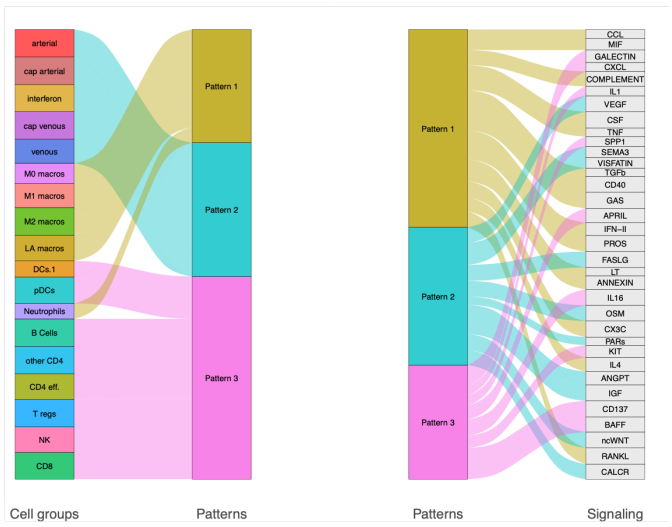
Incoming communication patterns of target cells
arterial
cap arterial
interferon
cap venous
venous
M0 macros
M1 macros
M2 macros
LA macros
DCs.1
pDCs
Neutrophils
B Cells
other CD4
CD4 eff.
T regs
NK
CD8
Pattern 1
Pattern 2
Pattern 3
CCL
MIF
GALECTIN
CXCL
COMPLEMENT
IL1
VEGF
CSF
TNF
SPP1
SEMA3
VISFATIN
TGFb
CD40
GAS
APRIL
IFN−II
PROS
FASLG
LT
ANNEXIN
IL16
OSM
CX3C
PARs
KIT
IL4
ANGPT
IGF
CD137
BAFF
ncWNT
RANKL
CALCR
Cell groups
Patterns
Patterns
Signaling

eFigure 12

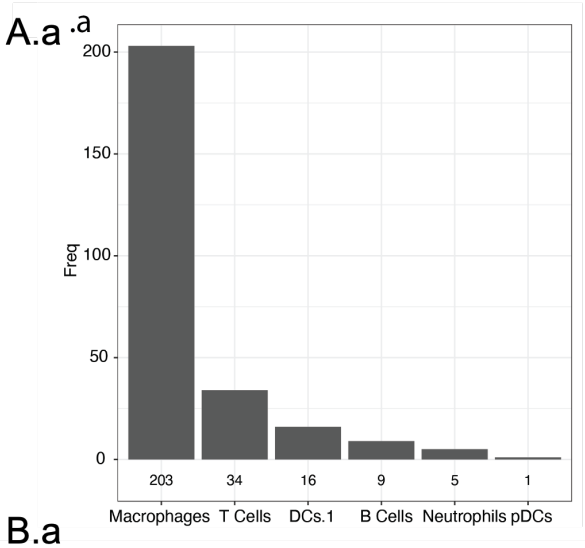
A.a
Freq
200
150
100
50
0
203
34
16
9
5
1
Macrophages
T Cells
DCs.1
B Cells
Neutrophils
pDCs

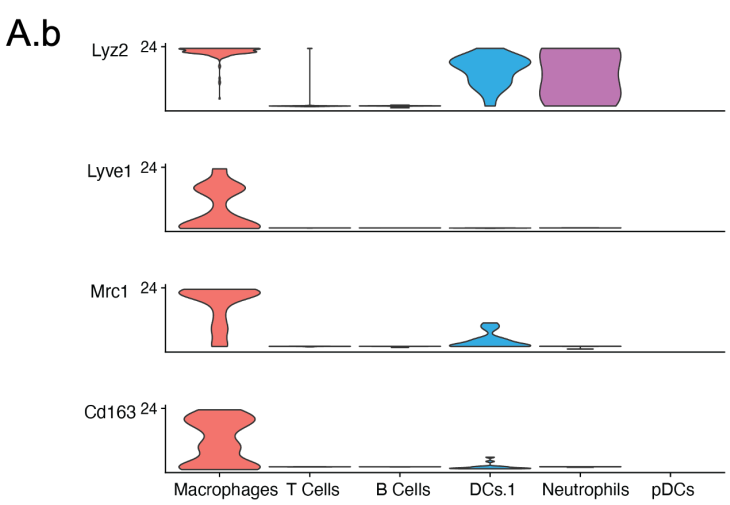
A.b
Lyz2
Lyve1
Mrc1
Cd163
24
Macrophages
T Cells
B Cells
DCs.1
Neutrophils
pDCs

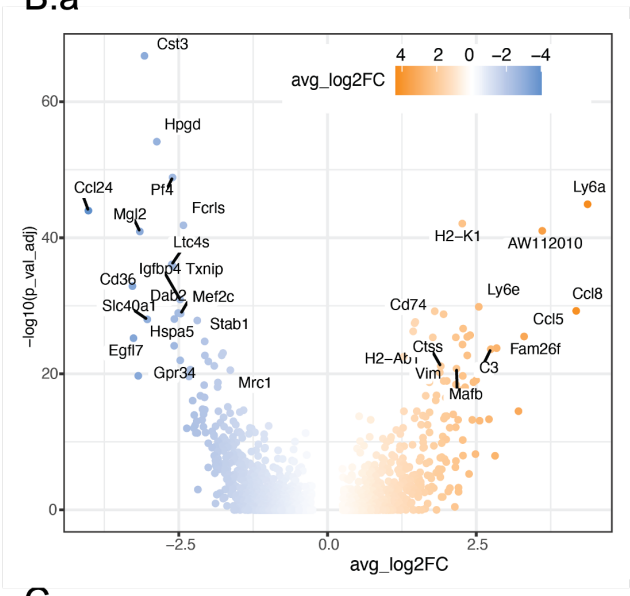
B.a
avg_log2FC
4
2
0
−2
−4
−log10(p_val_adj)
avg_log2FC
Cst3
Hpgd
Ccl24
Pf4
Mgl2
Fcrls
Ltc4s
Igfbp4
Txnip
Cd36
Dab2
Mef2c
Slc40a1
Stab1
Hspa5
Egfl7
Gpr34
Mrc1
Ly6a
H2−K1
AW112010
Ly6e
Ccl8
Cd74
Ccl5
Ctss
H2−Ab
Fam26f
C3
Vim
Mafb

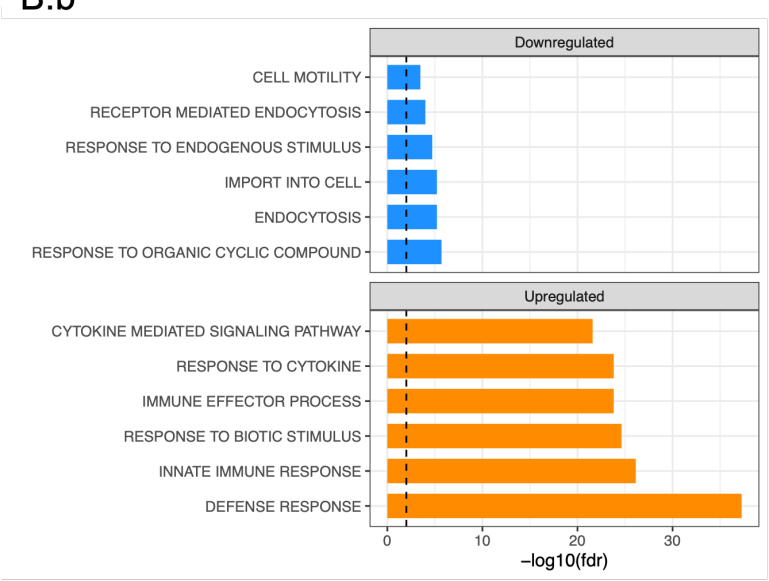
B.b
Downregulated
CELL MOTILITY
RECEPTOR MEDIATED ENDOCYTOSIS
RESPONSE TO ENDOGENOUS STIMULUS
IMPORT INTO CELL
ENDOCYTOSIS
RESPONSE TO ORGANIC CYCLIC COMPOUND
Upregulated
CYTOKINE MEDIATED SIGNALING PATHWAY
RESPONSE TO CYTOKINE
IMMUNE EFFECTOR PROCESS
RESPONSE TO BIOTIC STIMULUS
INNATE IMMUNE RESPONSE
DEFENSE RESPONSE
−log10(fdr)

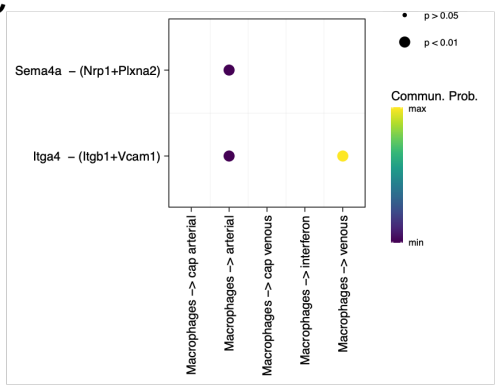
C
Sema4a − (Nrp1+Plxna2)
Itga4 − (Itgb1+Vcam1)
Commun. Prob.
p > 0.05
p < 0.01
Macrophages −> cap arterial
Macrophages −> arterial
Macrophages −> cap venous
Macrophages −> interferon
Macrophages −> venous

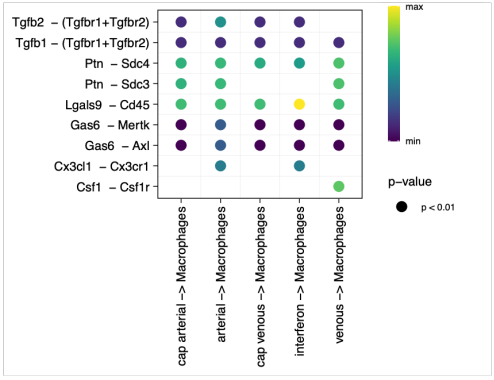
Tgfb2 − (Tgfbr1+Tgfbr2)
Tgfb1 − (Tgfbr1+Tgfbr2)
Ptn − Sdc4
Ptn − Sdc3
Lgals9 − Cd45
Gas6 − Mertk
Gas6 − Axl
Cx3cl1 − Cx3cr1
Csf1 − Csf1r
p−value
p < 0.01
cap arterial −> Macrophages
arterial −> Macrophages
cap venous −> Macrophages
interferon −> Macrophages
venous −> Macrophages

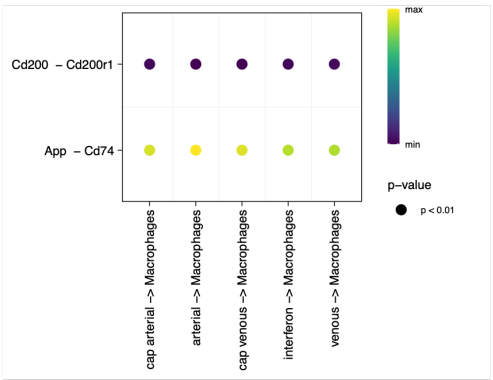
Cd200 − Cd200r1
App − Cd74
p−value
p < 0.01
cap arterial −> Macrophages
arterial −> Macrophages
cap venous −> Macrophages
interferon −> Macrophages
venous −> Macrophages

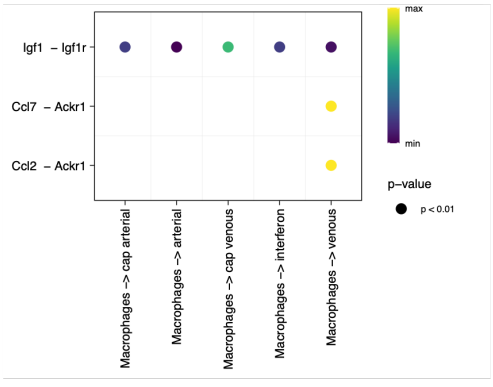
Igf1 − Igf1r
Ccl7 − Ackr1
Ccl2 − Ackr1
p−value
p < 0.01
Macrophages −> cap arterial
Macrophages −> arterial
Macrophages −> cap venous
Macrophages −> interferon
Macrophages −> venous

eFigure 13

eFIGURE LEGENDS:

eFigure 1. A) Distribution of QC metrics: Coverage (nCount_RNA), percentage of mitochondrial genes (percent.mt) and total number of genes (nFeature_RNA). Cells that were removed based on these values are colored in red. **B)** Comparison of QC across individual samples. **C)** Elbow plot showing the standard deviation of each PC from the total set dataset. This was used to decide how many PC dimensions were included for UMAP projection.

eFigure 2. A) Mapping of normalized expression for known different cell-type markers onto UMAP. **B)** Dot-plot of the top 5 genes with highest fold-changes when comparing a given cell-type to all other cells. Color gradient corresponds to mean normalized expression and the size of the dots show the percentage of cells from the cell-type of interest in which the gene is detected. DCs= dendritic cells; pDCs= plasmacytoid dendritic cells. **C)** Gene set enrichment network of the (41) shared up-regulated genes between endothelial cells, microglia, mature oligodendrocytes and astrocytes. **D)** Boxplot of the significantly upregulated genes shared by ECs, microglia, mature oligodendrocytes and astrocytes that showed the highest fold-changes in at least one of the four cell-types.

eFigure 3. A.a) UMAP and unsupervised cluster identity of microglia subpopulations. **A.b)** Proportions of microglia subpopulations across controls and EAE mice. **A.c)** Dot-plot of the top 5 genes identified as microglial subpopulation markers. The color gradient corresponds to mean normalized expression and the size of the dots shows the percentage of cells in which the gene is detected. **B.a)** UMAP and unsupervised cluster identity of mature oligodendrocytes. **B.b)** Proportions of each identified mature oligodendrocyte subpopulations across controls and EAE mice. **B.c)** Dot-plot of the top 5 genes identified as oligodendrocyte subpopulations markers. The color gradient corresponds to mean normalized expression and the size of the dots shows the

percentage of cells in which the gene is detected. **C.a)** UMAP and unsupervised cluster identity of astrocytes. **C.b)** Proportions of astrocyte subpopulations across controls and EAE mice. **C.c)** Dot-plot of the top 5 genes identified as astrocyte subpopulation markers. The color gradient corresponds to mean normalized expression and the size of the dots shows the percentage of cells in which the gene is detected.

eFigure 4. A) UMAP showing the cell clusters on CD31 selected cells. Cell-types were annotated with the 2021 Panglao cell-types gene sets from enrichR. **B)** Proportion of ECs with and without the CD31+ selection. **C)** Pie chart of the proportions of each identified cell population in the CD31+ selected samples.

eFigure 5. A.a) UMAP visualization of ECs clusters after integrating across both batch and condition to allow overlay of homologous structures despite condition-wise transcriptional differences. **A.b)** Dot-plot of the top 5 markers with highest fold-change when comparing each cluster with all other clusters. The color gradient corresponds to mean normalized expression and the size of the dots shows the percentage of cells in which the gene is detected. **A.c)** UMAP visualization of the enrichment for the genes associated with each ECs subtype using a cluster-level analysis. Each cluster is colored with the –log10(FDR) of its enrichment for a given geneset, as calculated by a fisher-test. **B.a)** Dot-plot of known arteriovenous zonation markers across ECs clusters. **B.b)** Dot plot of the mean value for calculated module scores for each cluster. **C)** Expression of arteriovenous zonation markers along pseudotime ranking. Each bar represents a cell. **D)** Proportion of ECs subtypes in EAE and control mice.

eFigure 6: A.a) UMAP projection of ECs from control and EAE mice colored by subtypes. **A.b)** UMAP visualization of ECs from CD31-selected cells, colored by disease condition (control vs EAE). **A.c)** UMAP visualization of ECs colored by clustering identity. **A.d)** Proportion of the different clusters among EC subpopulations. C= control; E=EAE. A.e) Relative proportion of each cluster across samples. Identifies cluster 2 as disease-specific.

B) Dot-plot of the top 5 genes identified as EC subpopulation markers. Color gradient corresponds to mean normalized expression and the size of the dots shows the percentage of cells in which the gene is detected. **C.a)** Gene set enrichment analysis of the biological pathways represented by the transcriptional changes shared by all ECs. **C.b)** Gene set enrichment analysis of the biological pathways represented by the specific transcriptional changes of venous ECs.

eFigure 7. A.a) Pseudotime of first lineage mapped on integrated UMAP. Arrow shows trajectory. **A.b)** Distribution of the relative importance of each gene in the random forest model with first pseudotime as outcome. Red vertical line shows threshold (top 5%) used to select genes displayed in C. **A.c)** UMAP colored by the expression of the genes associated with the first pseudotime trajectory. **B.a)** Pseudotime of second lineage mapped on integrated UMAP. Arrow shows trajectory. **B.b)** Distribution of the relative importance of each gene in the random forest model with second pseudotime as outcome. Red vertical line shows threshold (top 5%) used to select genes displayed in F. **B.c)** UMAP colored by the expression of the genes associated with the second pseudotime trajectory.

eFigure 8: A) mRNA expression of adhesion molecules and tight junction proteins along pseudotime ranking, separated by condition. Each bar represents a cell, and subtype identity is color-coded on the x-axis. **B)** Heatmap of log2 fold-changes for genes with known roles in BBB function and immune cell infiltration. Non-significant genes are displayed as grey tiles. (*p<0,05 ; **p<0,01 ; ***p<0,001).

eFigure 9. A) Expression of genes allowing lymphocyte subset identification mapped onto UMAP. Also, cell-cycle phase prediction and identified cell-type on the two last plots. Pie chart of the proportions of each identified lymphocyte population. **B)** Expression of genes allowing macrophage subset discrimination mapped onto UMAP, along with cell-cycle

phase prediction and identified cell-type on the two last plots. Pie chart of the proportions of each identified macrophage population.

eFigure 10: A) Expression of genes allowing immune subset identification onto UMAP. **B)** Dot-plot of the top 4 markers with highest fold-change when comparing each cell-type with all other cells. **C)** UMAP colored with the expression of Nectin2, CD226 and Tigit. **D)** UMAP colored with the expression of Ackr1, Ccl7 and Ccl8.

eFigure 11. A.a) Dot-plot summarizing probability of interactions between venous ECs and immune subsets through secreted signaling. **A.b)** Dot-plot summarizing probability of interactions between venous ECs and immune subsets through cell-cell contact. **B.a)** Violin plots showing the expression of CCLs involved in potential interactions across all cell-types. **B.b)** Violin plots of CXCLs expression across cell types. **C)** Circos plot showing interaction pathways involving CCLs and CXCLs cytokines secreted by immune subsets and receptors expressed by ECs.

eFigure 12. Grouping of cell-types based on their patterns of outgoing and incoming interactions. As suggested by *CellChat*, the total number of patterns was determined by inspecting the Cophenetic and Silhouette values.

eFigure 13. A.a) Number of cells across immune cell-types in control mice. **A.b)** Violin plots showing the expression of known markers of resident macrophages. **B.a)** Volcano plots showing differential expression testing for all genes between resident macrophages from EAE and control mice. **B.b)** Gene set enrichment analysis of the biological pathways represented by the transcriptional changes between resident macrophages in control and EAE mice. **C)** Dot-plot summarizing probability of interactions between ECs and resident macrophages in control mice.